J. Membrane Biol. 117, 11–27 (1990)

The Journal of
Membrane Biology
© Springer-Verlag New York Inc. 1990

Presteady-State Kinetics and Carrier-Mediated Transport: A Theoretical Analysis

Wieslaw Wierzbicki†, Alfred Berteloot‡, and Guy Roy†
Groupe de Recherche en Transport Membranaire, †Département de Physique et ‡Département de Physiologie, Université de Montréal, C.P. 6128, Succursale A, Montréal, Québec, Canada H3C 3J7

Summary. Kinetic studies of cotransport mechanisms have so far been limited to the conventional steady-state approach which does not allow in general to resolve either isomerization or rate-limiting steps and to determine the values of the individual rate constants for the elementary reactions involved along a given transport pathway. Such questions can only be answered using presteady-state or relaxation experiments which, for technical reasons, have not yet been introduced into the field of co-transport kinetics. However, since two recent reports seem compatible with the observation of such transient kinetics, it would appear that theoretical studies are needed to evaluate the validity of such claims and to critically evaluate the expectations from a presteady-state approach. We thus report such a study which was performed on a simple four-state mechanism of carrier-mediated transport. The time-dependent equation for zero-*trans* substrate uptake was thus derived and then extended to models with p intermediary steps. It is concluded that $(p - 1)$ exponential terms will describe the approach to the steady state but that such equations have low analytical value since the parameters of the flux equation cannot be expressed in terms of the individual rate constants of the elementary reactions for models with $p > 5$. We thus propose realistic simplifications based on the time-scale separation hypothesis which allows replacement of the rate constants of the rapid steps by their equilibrium constants, thereby reducing the complexity of the kinetic system. Assuming that only one relaxation can be observed, this treatment generates approximate models for which analytical expressions can easily be derived and simulated through computer modeling. When performed on the four-state mechanism of carrier-mediated transport, the simulations demonstrate the validity of the approximate solutions derived according to this hypothesis. Moreover, our approach clearly shows that presteady-state kinetics, should they become applicable to (co)transport kinetics, could be invaluable in determining more precise transport mechanisms.

Key Words carrier-mediated transport · presteady-state · kinetic models · rapid equilibrium approximation · zero-*trans* influx kinetics · membrane vesicles

Introduction

In a recent paper, we have re-evaluated the electrogenicity of glutamic acid transport in brush-border membrane vesicles isolated from the rabbit small intestine and our results clearly demonstrated that the rheogenic character of the transport system was determined by both the ionic environment and the surrounding pH (Berteloot, 1986). During these studies, it was also observed that downward and upward curvatures were introduced in the time courses of glutamic acid uptake by inside-negative and inside-positive membrane potentials, respectively, while uptake was linear during the first minute at zero potential. Such deviations from linearity, which seem to correlate with the size and polarity of the membrane potential, could thus indicate the presence of transient states before the establishment of a true steady state at each of the applied potentials. According to this hypothesis and to the nomenclature currently used to describe the prestationnary phases, lag (acceleration in the uptake rate before reaching the steady state) and burst (the reverse process) kinetics would have been observed with positive and negative membrane potentials, respectively. Obviously, in the absence of a true linear part being observed in the uptake time courses, the difference between a burst-like transient and a deviation from true initial rate conditions may be quite impossible to resolve under the so-called zero-*trans* gradient conditions in vesicle studies (Hopfer et al., 1973). This is so because of the transient nature of the electrochemical gradients for both the substrate and the cotransported ion which may lead rapidly to uptake inhibition by intravesicular product accumulation and/or collapse of the driving forces (Hopfer, 1977; Hopfer & Groseclose, 1980; Dorando & Crane, 1984; Semenza et al., 1984). The situation is, however, different for lag-like transients which cannot be produced by the above mechanism. Other possible explanations involving temperature, buffer, and pH effects following the addition of the vesicle suspension to the uptake medium are easily ruled out in our experiments as these factors have been readily

controlled. It would thus appear that the lag-like situations may well represent a true transient situation (presteady-state) occurring before the establishment of the steady state. Similar conclusions have been reached recently by Otsu et al. (1989) while measuring the kinetics of ^{22}Na uptake through the Na^+-H^+ exchange transport system of rabbit renal brush-border membrane vesicles. In this case, transient phases corresponding to lag and burst have been observed before reaching a linear uptake period, thus indicating that true relaxations occur before the establishment of the steady state.

So far, the conventional approach to the study of cotransport kinetics in brush-border membrane vesicles has been to measure initial rates of transport (but *see* Semenza et al. (1984) for a critical appraisal of such practice) and to apply steady-state methods in the derivation of kinetic equations for cotransport models. The earlier view of a mobile carrier type of mechanism (Crane, 1977) has led to consider that thermodynamical constraints must limit the mobility of large, intramembrane proteins and such considerations gave a physical basis to the notion that carrier-mediated transport is rate limited at the translocation steps. A rapid equilibrium assumption in the kinetic treatment of the steady-state approach was thus indirectly justified. Moreover, the simplifications that could be introduced in the derivation of the rate equations and the relatively simple analytical expressions of the rate laws contributed greatly to the popularity of this hypothesis (Schultz & Curran, 1970; Heinz, Geck & Wilbrandt, 1972; Jacquez, 1972; Kimmich & Carter-Su, 1978; Turner, 1981, 1983, 1985). In these deviations, other assumptions as to the symmetry of translocation rate constants (Schultz & Curran, 1970), symmetry of binding events at the two membrane faces (Jacquez, 1972), and lack of mobility of partially loaded forms of the carrier (Kimmich & Carter-Su, 1978) have also been made to reduce the analytical expressions of the rate laws but lack experimental support and have even been dismissed (Hopfer & Groseclose, 1980; Dorando & Crane, 1984; Semenza et al., 1984). The now accepted view that intrinsic membrane proteins that span the membrane lipid bilayer may well account for membrane transport properties (Hopfer & Groseclose, 1980; Crane & Dorando, 1984; Semenza et al., 1984) has raised questions as to the validity of this assumption which was sometimes released in the derivation of steady-state models (Stein, 1976; Stein & Honig, 1977; Sanders et al., 1984; Harrison et al., 1985; Sanders, 1986). An interesting conclusion of such analysis is that simple models lacking that assumption turn out to be highly flexible and are able to describe most of the kinetic diversity observed in co- and counter-transport systems (Sanders et al., 1984). It also led to the speculation that the observed diversity in cotransport kinetics reflects a control-related selection of reaction rate constants rather than fundamental differences in mechanisms (Sanders et al., 1984).

Since steady-state rate laws are relatively easy to derive and give analytical solutions, they may usually be cast into a form which is convenient for the experimental determination of a number of characteristic kinetic parameters by standard curve-fitting procedures. These are, however, complicated functions of the individual rate constants for the elementary steps along a transport pathway which cannot be determined in general for any realistic mechanism. Only lower bound values to the rate constants of individual reactions and order of substrate addition in multiple substrate, multiple product reactions can be obtained (Hopfer & Groseclose, 1980; Dorando & Crane, 1984; Semenza et al., 1984) by the steady-state approach. Experimental simplifications can, however, be devised as to allow an estimation of some of these rate constants (Sanders, 1986). Nevertheless, it has also been appreciated that presteady-state methods and transient-state kinetics would be invaluable in leading to the detailed understanding of the mechanism of active transport (Stein & Honig, 1977).

It is by now well established in the field of enzymology that rapid kinetics and relaxation experiments (Hammes & Schimmel, 1970) are complementary approaches that can contribute to resolve complex kinetic mechanisms. So far, their applications to membrane transport studies have only been possible with black lipid membranes containing ion carriers like valinomycin and nonactin (Stark et al., 1971; Laprade et al., 1975). These simple models could be solved analytically and fully characterized from the measurement data. In the case of cotransport systems, the absence of fast sampling methods and of techniques allowing continuous recording of rapid reactions are the main obstacles which have precluded such an experimental approach and may even have masked the possible observation of presteady-state kinetics. However, as discussed in the first paragraph, recent findings with glutamic acid transport (Berteloot, 1986) and Na^+-H^+ exchange (Otsu et al., 1989) are difficult to explain within the framework of the steady-state analysis. It is thus the purpose of the present paper to explore the compatibility of these observations with the predictions from a theoretical treatment of presteady-state kinetics as applied to transport mechanisms. Moreover, our approach aims at finding an analytical formulation describing these presteady-states, a strategy which is different from the one of Otsu et al. (1989) who have only conducted a numerical analysis of their data.

In the present paper, we tried to answer the following questions: (*i*) What kind of transient kinetics can we expect to observe when dealing with transport mechanisms? (*ii*) How will the number and the position of the rate-limiting steps along a transport pathway influence the transient kinetics? (*iii*) How will the substrate concentrations and the membrane potential affect the transient kinetics? (*iv*) Is it possible to discriminate between concurrent models from the experimental observation of presteady-state kinetics? For this purpose, we first analyze a simple four-state model of carrier-mediated transport and derive the general equation for substrate flux. We next discuss the limitations of presteady-state kinetics when extending this solution to cotransport systems with an arbitrary number of intermediary steps. We then propose realistic simplifications that would allow establishment of approximate analytical solutions for models involving different number and position of rate-limiting steps and these are applied to the four-state model of carrier-mediated transport. Finally, simulations are performed in order to justify the proposed simplifications and to assess substrate and membrane potential effects in the case of a special model with rapid equilibrium surface reactions.

Theory

Basic Model and General Assumptions

In order to study the relation between substrate flux and transition rates, we used the conventional carrier model for carrier-mediated transport (Widdas, 1952; Geck & Heinz, 1981) with the notations shown in Fig. 1. The following assumptions concerning the transport process and the experimental conditions under which fluxes are measured are made.

Carrier Assumption

The binding site for the transported ligand X on the carrier N is only accessible from one side of the membrane at a time and its transmembrane reorientation in either the unloaded state (N_1–N_2 transition) or as a substrate-carrier complex (N_3–N_4 transition) is a first-order process. Moreover, since no assumption regarding the energetics of the transport events is made, this model should be equally applicable to both active and passive transport systems (Geck & Heinz, 1981). In this context, it is interesting to note that the transport model shown in Fig. 1 also corresponds to the basic model for cotransport as proposed by Crane (1977).

Conservation of Carriers

The total number of carriers is constant and equal to N_T. It is thus possible to write down the conservation Eq. (1) corresponding to the model of Fig. 1.

$$N_T = N_1 + N_2 + N_3 + N_4. \tag{1}$$

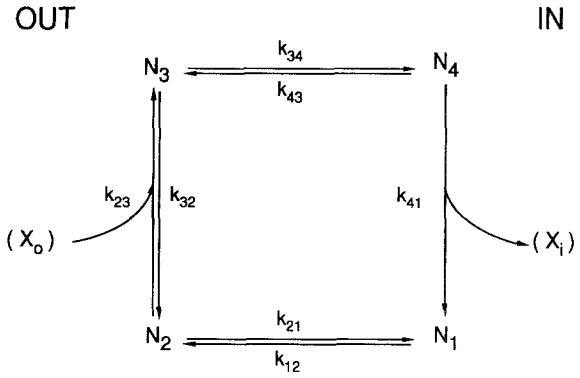

Fig. 1. Basic model for carrier-mediated transport of substrate X by carrier N used in our study. Assumptions are discussed in the text

Zero-Trans Influx Conditions

The following studies will be limited to zero-*trans* influx experiments in which the transport assay is started by mixing a radioactive substrate with vesicles pre-equilibrated in a substrate-free medium. Under such conditions, the boundary conditions at $t = 0$ (mixing time) for the concentrations of the different carrier forms denoted as N_j^* are determined by Eqs. (2) and (3).

$$N_3^* = N_4^* = 0 \tag{2}$$

$$k_{12}N_1^* = k_{21}N_2^*. \tag{3}$$

The concentrations of inside- and outside-facing carriers N_1^* and N_2^* present at the start of the experiment are thus easily calculated by solving simultaneously Eqs. (1) to (3) and correspond to Eqs. (4) and (5), respectively.

$$N_1^* = \frac{k_{21}N_T}{k_{12} + k_{21}} \tag{4}$$

$$N_2^* = \frac{k_{12}N_T}{k_{12} + k_{21}}. \tag{5}$$

It is assumed that the zero-*trans* conditions, as defined by Eq. (6), are maintained during the time period over which the measurements are made.

$$(X_i)|_{t=0} = 0. \tag{6}$$

Accordingly, the contribution of efflux to the net transport rate is negligible so that unidirectional zero-*trans* entry rates are actually measured and can be calculated from Eq. (7).

$$\frac{d(X_i)}{dt} = k_{41}N_4. \tag{7}$$

Other Assumptions

Implicit in this paper is the assumption that the volume of the external medium is infinite as compared to the intravesicular volume, so that the variations in external substrate concentrations can be neglected. It should be noted that a similar approxi-

mation could be made in other preparations provided that inequation (8) is satisfied.

$$(X_o) \gg N_T. \tag{8}$$

Finally, it is assumed that binding does not contribute significantly to the measured uptake, so that $X_i(t)$ can be approximated to represent the total uptake process.

Formal Development of the Basic Model

Under zero-*trans* conditions where Eq. (6) applies, the basic model presented in Fig. 1 is associated with the set of differential Eqs. (9)–(12) which expresses the time dependence of the N_j carrier forms.

$$\frac{dN_1}{dt} = -k_{12}N_1 + k_{21}N_2 + k_{41}N_4 \tag{9}$$

$$\frac{dN_2}{dt} = k_{12}N_1 - [k_{21} + k_{23}(X_o)]N_2 + k_{32}N_3 \tag{10}$$

$$\frac{dN_3}{dt} = k_{23}(X_o)N_2 - (k_{32} + k_{34})N_3 + k_{43}N_4 \tag{11}$$

$$\frac{dN_4}{dt} = k_{34}N_3 - (k_{41} + k_{43})N_4. \tag{12}$$

Since the conservation Eq. (1) can be introduced into Eqs. (9)–(12) such as to eliminate any one of these, the problem thus resumes at solving a set of three inhomogeneous linear differential equations. The solution of such systems is represented by the solution of the corresponding homogeneous system plus a particular solution of the inhomogeneous system which is given by the steady-state concentration N_j^s obtained by setting $dN_j/dt = 0$ into Eqs. (9)–(12). The general solution will thus be identical in form to a solution previously derived by Stark et al. (1971) and corresponds to Eq. (13) for which the boundary conditions at $t = 0$ are represented by Eqs. (2), (4) and (5).

$$N_j = \sum_{k=1}^{3} C_j^k \exp(-\alpha_k t) + N_j^s. \tag{13}$$

In Eq. (13), the 12 C_j^k terms are the amplitudes for the relaxation of the different carrier forms and can be evaluated as proposed by Stark et al. (1971). The three α_k's represent the reverse of the time constants for these different relaxations and are the roots of the characteristic polynomial of the homogeneous system.

The general solution for substrate uptake will thus take the form of Eq. (14) which is obtained by integration of Eq. (7) with boundary conditions corresponding to Eq. (6) and where N_4 is given by Eq. (13).

$$(X_i) = \sum_{k=1}^{3} A_k \exp(-\alpha_k t) + Bt - A. \tag{14}$$

In Eq. (14), the α_k's have the same meaning and expressions as in Eq. (13) while the A_k's represent the amplitudes of the different relaxations as seen by measuring substrate uptake and satisfy Eq. (15).

$$A = \sum_{k=1}^{3} A_k. \tag{15}$$

It must be noted that it is the sign of the amplitude terms which determines the nature of the transient state to be observed with lags (upward deviations) and bursts (downward deviations) corresponding to $A > 0$ and $A < 0$, respectively. Finally, in Eq. (14), the B term is the steady-state influx and represents the quantity which is usually measured by the slope of a straight line during the early period of the uptake time course. Its expression is given by Eq. (16).

$$B = k_{41}N_4^S. \tag{16}$$

Generalization: Application to Cotransport Models and Limitations of the Presteady-State Approach

Although the model presented in Fig. 1 corresponds to the basic model of cotransport as proposed by Crane (1977), it lacks the power of its more expanded forms (Crane, 1977; Crane & Dorando, 1984; Turner, 1981) since it does not account for the order of addition of substrate and ion and for the stoichiometry (n, number of ions cotransported with one molecule of substrate) of the cotransport mechanism. It thus becomes obvious that the basic model of Fig. 1 may well account for cotransport mechanisms but under very restrictive conditions only.

Since a more realistic description of cotransport mechanisms will have to consider models with varying numbers of p intermediary steps, it becomes interesting to briefly comment on what can be expected from presteady-state measurements in such systems. The formal development of complex models will be similar to the one proposed above in the case of the basic model and thus should lead to a set of p differential equations with their corresponding boundary conditions and conservation equation. The problem would in fact resume at solving a set of $(p - 1)$ inhomogeneous linear differential equations, the general solution of which is similar to Eq. (13) with $p(p - 1)$ amplitude terms and $(p - 1)$ relaxation constants. The whole process will thus require to solve for a polynomial of degree $(p - 1)$ for which no analytical solution can actually be extracted if $p > 5$. The conclusion is that the analysis of such kinetic systems far from equilibrium will be hampered by the inherent mathematical limitations of treating transient states in an analytical way, a shortcoming that can only be overcome by obtaining numerical solutions to the differential equations with an analog or digital computer. When applied to complex mechanisms, such an approach will be most powerful in simulating systems for which the values of the rate constants for the various steps are at least approximately known. However, if one wants to determine these rate constants, it becomes quite impossible to find a unique set of parameters that will reproduce the experimental data.

From the above discussion, it appears that trying to overcome the mathematical difficulty by finding some acceptable simplifications may prove more gratifying than trying to solve it. In an attempt to find such a compromise that may be applicable to even complex models, we started by considering that all of the transient states might not be observable at the same time or, alternatively, that experimental conditions can always be set up such as to limit the number of observable transient states. In other words, it seemed appropriate to introduce approximations based on the principle that some of the reaction steps are faster than others, so that relaxations to be observed on a given time scale can be limited to the slowest ones. Moreover, since the time resolution achieved with most of these methods has so far not allowed the observation of more than one (Berteloot, 1986) or two (Otsu et al., 1989) of the $(p - 1)$ transient states predicted

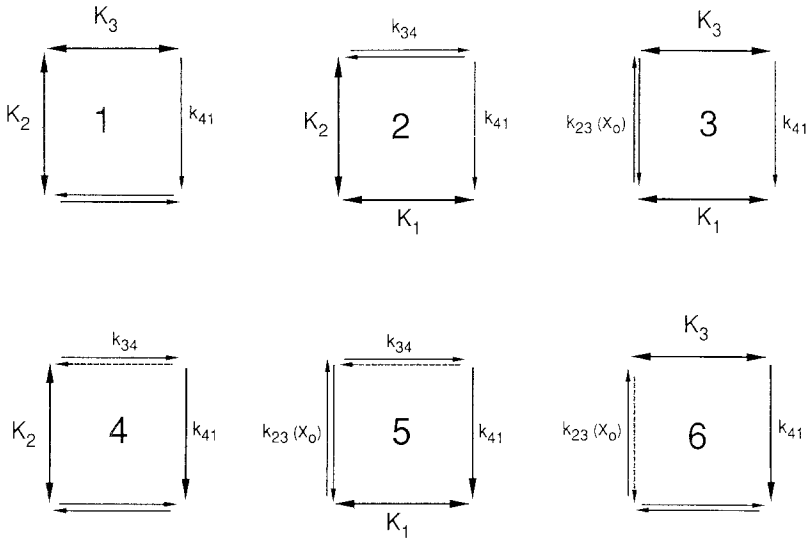

Fig. 2. Approximate models generated from the basic model of Fig. 1 assuming two rapid steps in different locations along the transport cycle (thick arrows). *See* text for more details

by a generalized Eq. (14), it is interesting to first limit ourselves to the case where only one transient state is observed with the basic model of Fig. 1. The first part of Results will consider such an approach in more details while the second will use the analytical solutions so generated to simulate both substrate and membrane potential effects in order to determine a strategy for model discrimination.

Results

Approximate Models with One Transient State

The Separation of Time-Scale Hypothesis

In the following, and for reasons discussed in the previous section, we assume that only one transient state can be observed under the conditions of a given experiment. In other words, this hypothesis is equivalent to saying that the various decay processes occur at vastly different rates and that only the slow relaxations can be observed. This simple assertion allows establishment of the rationale for the presteady-state treatment which is developed in this section and can be viewed as follows. At the start of the transport assay and over a time period short enough as compared to the time constants of the slowly relaxing steps, all carrier forms linked by rapid steps will redistribute before any substantial uptake can be observed. It is thus possible to define new initial conditions that will be established before the start of the observable relaxation process and to study the approach toward the steady state from these new initial conditions.

Given that only one relaxation can be observed, it is readily apparent from Eq. (13) that such a hypothesis is compatible with only two slow steps being present along the transport cycle of the carrier model shown in Fig. 1, a condition that is satisfied by the six possible models presented in Fig. 2. As shown, these six models are under the configuration corresponding to the new initial conditions defined above. Accordingly, whenever rapid steps are present, it is legitimate to introduce a rapid equilibrium assumption in which the rate constants of the rapid steps can be replaced by equilibrium constants (K_j) as defined by Eqs. (17) to (19).

$$K_1 = \frac{k_{21}}{k_{12}} = \frac{N_1}{N_2} \tag{17}$$

$$K_2 = \frac{k_{32}}{k_{23}} = \frac{N_2(X_o)}{N_3} \tag{18}$$

$$K_3 = \frac{k_{43}}{k_{34}} = \frac{N_3}{N_4}. \tag{19}$$

It should be noted, however, that such a relationship cannot be established for the substrate-releasing step on the internal side because of the zero-*trans* conditions defined by Eq. (6). It now becomes possible to estimate the new carrier distribution N_j^o that will serve as initial boundary conditions for the integration of the time-dependent variation of the different carrier forms in all of the approximate models shown in Fig. 2.

In the configuration of model *1* of Fig. 2, the addition of substrate at time $t = 0$ will allow fast redistribution of carrier form N_2^* as defined by Eq. (5) between the three forms N_2^o, N_3^o and N_4^o while form N_1^* as defined by Eq. (4) cannot redistribute. Equations (20) and (21) will thus apply and can be solved for all N_j^o by introducing Eqs. (5), (18) and (19) into Eq. (21).

Table 1. Initial carrier distribution resulting from the rapid equilibrium treatment of presteady-state kinetics to carrier-mediated transport under zero-*trans* conditions as applied to the different models of Fig. 2

Model	N_1^o	N_2^o	N_3^o	N_4^o
(1)	$\frac{k_{21}N_T}{k_{12}+k_{21}}$	$\frac{k_{12}K_2K_3N_T}{(k_{12}+k_{21})[K_2K_3+(1+K_3)(X_o)]}$	$\frac{k_{12}K_3N_T(X_o)}{(k_{12}+k_{21})[K_2K_3+(1+K_3)(X_o)]}$	$\frac{k_{21}N_T(X_o)}{(k_{12}+k_{21})[K_2K_3+(1+K_3)(X_o)]}$
(2)	$\frac{K_1K_2N_T}{(1+K_1)K_2+(X_o)}$	$\frac{K_2N_T}{(1+K_1)K_2+(X_o)}$	$\frac{N_T(X_o)}{(1+K_1)K_2+(X_o)}$	0
(3)	$\frac{K_1N_T}{(1+K_1)}$	$\frac{N_T}{(1+K_1)}$	0	0
(4)	$\frac{k_{21}N_T}{k_{12}+k_{21}}$	$\frac{k_{12}K_2N_T}{(k_{12}+k_{21})[K_2+(X_o)]}$	$\frac{k_{12}N_T(X_o)}{(k_{12}+k_{21})[K_2+(X_o)]}$	0
(5)	$\frac{K_1N_T}{(1+K_1)}$	$\frac{N_T}{(1+K_1)}$	0	0
(6)	$\frac{k_{21}N_T}{k_{12}+k_{21}}$	$\frac{k_{12}N_T}{k_{12}+k_{21}}$	0	0

$$N_1^o = N_1^* \tag{20}$$

$$N_2^o + N_3^o + N_4^o = N_2^*. \tag{21}$$

In the case of model *2* of Fig. 2, substrate addition will produce the fast redistribution of carrier forms N_1^* and N_2^* into carrier forms N_1^o, N_2^o and N_3^o, so that Eq. (22) will apply which can be solved by introducing Eqs. (17) and (18).

$$N_1^o + N_2^o + N_3^o = N_1^* + N_2^* = N_T. \tag{22}$$

In the case of model *4* of Fig. 2, only form N_2^* can redistribute and Eqs. (20) and (23) will apply, the last one being solved with the help of Eq. (18).

$$N_2^o + N_3^o = N_2^*. \tag{23}$$

In the case of models *3*, *5* and *6* of Fig. 2, neither form N_1^* nor N_2^* can redistribute, so that Eqs. (20), (24) and (25) will apply. However, in the case of models *3* and *5*, Eq. (17) needs to be introduced into Eqs. (20) and (25) where N_1^* and N_2^* are given by Eqs. (4) and (5), respectively.

$$N_3^o = N_4^o = 0 \tag{24}$$

$$N_2^o = N_2^*. \tag{25}$$

The solutions for the N_j^o in each of the six possible models of Fig. 2 are summarized in Table 1. Having so defined the initial boundaries (represented by the N_j^o) of the relaxation process, it now becomes possible to derive the rate equations for each of the approximate models in order to find out their characteristic analytical solutions.

Solution of Approximate Models 1–3: The Rapid Equilibrium Treatment

In the case of models *1–3*, the set of Eqs. (9)–(12) can be reduced by introducing the equilibrium constants relevant to each specific model and the conservation Eq. (1), thus leaving only one differential equation to integrate. The details of the calculations are only shown in the case of model *1* but are similar for models *2* and *3*. Equations (18) and (19) can first be derived to give Eqs. (26) and (27) from which Eq. (28) can be established by taking into account the derivative of the conservation Eq. (1).

$$K_2 \frac{dN_3}{dt} = (X_o) \frac{dN_2}{dt} \tag{26}$$

$$K_3 \frac{dN_4}{dt} = \frac{dN_3}{dt} \tag{27}$$

$$\frac{dN_2}{dt} + \frac{dN_3}{dt} + \frac{dN_4}{dt} = \frac{dN_4}{dt}\left[1 + K_3 + \frac{K_2K_3}{(X_o)}\right] = -\frac{dN_1}{dt}. \tag{28}$$

Since the value of dN_1/dt is given by Eq. (9) in which the values of N_1 and N_2 can be expressed as a function of N_4 through Eqs. (1), (18) and (19), Eq. (28) can be rearranged to give Eq. (29).

$$\frac{dN_4}{dt} = \frac{k_{12}N_T(X_o)}{K_2K_3 + (1+K_3)(X_o)} - N_4\left\{\frac{K_2K_3(k_{12}+k_{21}) + [k_{41}+k_{12}(1+K_3)](X_o)}{K_2K_3 + (1+K_3)(X_o)}\right\}. \tag{29}$$

Equation (29) can be cast under the form of Eq. (30) where α is the coefficient of N_4 under brackets

Table 2. Equations for the relaxation amplitude (A) of the transient state corresponding to models of Fig. 2 under zero-*trans* conditions

Model	Relaxation amplitude (A)
(1)	$\frac{k_{12}k_{41}[k_{21}(1 + K_3) - k_{41}]N_T(X_o)^2}{(k_{12} + k_{21})[(k_{12} + k_{21})K_2K_3 + [k_{12}(1 + K_3) + k_{41}](X_o)]^2}$
(2)	$\frac{k_{34}k_{41}N_T[(1 + K_1)K_2 + (X_o)](X_o)}{[(k_{41} + k_{43})(1 + K_1)K_2 + (k_{34} + k_{41} + k_{43})(X_o)]^2}$
(3)	$\frac{k_{23}k_{41}(1 + K_1)(1 + K_3)N_T(X_o)}{[(k_{32}K_3 + k_{41})(1 + K_1) + (1 + K_3)k_{23}(X_o)]^2}$
(4)	$\frac{k_{12}k_{34}(k_{21} - k_{34})N_T(X_o)^2}{(k_{12} + k_{21})[(k_{12} + k_{21})K_2 + (k_{12} + k_{34})(X_o)]^2}$
(5)	$\frac{k_{23}k_{34}(1 + K_1)K_1N_T(X_o)}{[(k_{32} + k_{34})(1 + K_1) + k_{23}(X_o)]^2}$
(6)	$-\frac{k_{12}(k_{23})^2N_T(X_o)^2}{(k_{12} + k_{21})[k_{12} + k_{21} + k_{23}(X_o)]^2}$

in Eq. (29) while N_4^S is the steady-state concentration of N_4 which is obtained by setting Eq. (29) equal to zero.

$$\frac{dN_4}{dt} + \alpha N_4 = \alpha N_4^S. \tag{30}$$

Equation (30) can now be integrated within the initial boundary limits given in Table 1 for model *1* and the final ones given by N_4^S to give Eq. (31) in which α is the inverse of the time constant for the relaxation process.

$$N_4 = N_4^S - (N_4^S - N_4^o)e^{-\alpha t}. \tag{31}$$

The rate expression for substrate uptake can then be calculated by integrating Eq. (7) in which N_4 is given by Eq. (31) to give Eq. (32) in which A represents the amplitude of the measured relaxation and is given by Eq. (33) while the B term is the steady-state influx given by Eq. (16). The α term has the same meaning as above.

$$(X_i) = Ae^{-\alpha t} + Bt - A \tag{32}$$

$$A = \frac{k_{41}(N_4^S - N_4^o)}{\alpha}. \tag{33}$$

The values of A and B in terms of the rate constants and equilibrium constants of model *1* can then be calculated from the known expressions of N_4^o, N_4^S, and α and are shown in Tables 2 and 3, respectively. Similar considerations apply to models *2* and *3* and equations similar to Eqs. (30) and (32) are obtained for which the respective values of A, B and $1/\alpha$ are shown in Tables 2 to 4.

Table 3. Equations for the steady-state influx of substrate (B) corresponding to models of Fig. 2 under zero-*trans* conditions

Model	Steady-state influx (B)
(1)	$\frac{k_{12}k_{41}N_T(X_o)}{(k_{12} + k_{21})K_2K_3 + [k_{12}(1 + K_3) + k_{41}](X_o)}$
(2)	$\frac{k_{34}k_{41}N_T(X_o)}{(k_{41} + k_{43})(1 + K_1)K_2 + (k_{34} + k_{41} + k_{43})(X_o)}$
(3)	$\frac{k_{23}k_{41}N_T(X_o)}{(k_{32}K_3 + k_{41})(1 + K_1) + (1 + K_3)k_{23}(X_o)}$
(4)	$\frac{k_{12}k_{34}N_T(X_o)}{(k_{12} + k_{21})K_2 + (k_{12} + k_{34})(X_o)}$
(5)	$\frac{k_{23}k_{34}N_T(X_o)}{(k_{32} + k_{34})(1 + K_1) + k_{23}(X_o)}$
(6)	$\frac{k_{12}k_{23}N_T(X_o)}{k_{12} + k_{21} + k_{23}(X_o)}$

Table 4. Equations for the time constant ($1/\alpha$) of the transient state corresponding to models of Fig. 2 under zero-*trans* conditions

Model	Time constant ($1/\alpha$)
(1)	$\frac{K_2K_3 + (1 + K_3)(X_o)}{(k_{12} + k_{21})K_2K_3 + [k_{12}(1 + K_3) + k_{41}](X_o)}$
(2)	$\frac{(1 + K_1)K_2 + (X_o)}{(1 + K_1)(k_{41} + k_{43})K_2 + (k_{34} + k_{41} + k_{43})(X_o)}$
(3)	$\frac{(1 + K_1)(1 + K_3)}{(k_{32}K_3 + k_{41})(1 + K_1) + k_{23}(1 + K_3)(X_o)}$
(4)	$\frac{K_2 + (X_o)}{(k_{12} + k_{21})K_2 + (k_{12} + k_{34})(X_o)}$
(5)	$\frac{1 + K_1}{(k_{32} + k_{34})(1 + K_1) + k_{23}(X_o)}$
(6)	$\frac{1}{k_{12} + k_{21} + k_{23}(X_o)}$

It is interesting to note from Eq. (33) that the value and the sign of A depend on the concentrations of N_4 which are achieved both during the final steady state (N_4^S) and immediately following the rapid redistribution of initial carrier forms (N_4^o). Actually, it is clear that the nature of the transient state to be observed depends on whether the rapid initial redistribution of carrier leads to N_4^o concentrations greater (burst) or smaller (lag) than the final steady-state concentration N_4^S. Accordingly, Table 2 shows that the sign of A is always positive for models *2* and *3* ($N_4^o = 0$), and so, that only lags are to be expected under these model configurations. On the contrary, for model *1*, the amplitude term can be either positive, negative, or nul, and so, either lag, burst, or absence of transient state may be obtained.

Solution of Approximate Models 4–6: The Steady-State Treatment

In models *4* and *5* of Fig. 2, one of the fast reactions involves the substrate debinding step on the internal side. In both cases, the rate of decomposition of N_4 is faster than its rate of formation so that whatever is formed can react immediately and no significant concentration will develop during both the relaxation process and during the steady state. This will be true until sufficient internal substrate can be accumulated such as to invalidate the zero-*trans* approximation which makes the N_4 to N_1 transition irreversible. These considerations have three important implications: (*i*) the concentration of N_4 will always be negligible, and, as such, it can be eliminated from the conservation Eq. (1); (*ii*) the slow transition from N_4 to N_3, which is governed by the slow rate constant k_{43} and the low concentration of N_4, becomes practically inexistent and can also be neglected (dashed lines in models *4* and *5* of Fig. 2); and (*iii*) because N_4 will decompose almost immediately upon formation, the three other carrier forms constitute a reservoir which slowly converts to N_4. The net effect of these two opposing processes is that a steady-state population of N_4 will prevail during the relaxation process, so that Eq. (12) can be set equal to zero. It should be emphasized that this steady-state assumption does not demand that $dN_4/dt = 0$, but, rather, it asserts that the net rate of change of N_4, dN_4/dt, is much smaller than either its instantaneous rate of formation or its instantaneous rate of decomposition. Neither of the latter two quantities need to be small, only their difference.

By introducing the last two simplifications into Eq. (12), it follows that the concentration of N_4 is always directly proportional to the concentration of N_3 according to Eq. (34).

$$N_4 = \frac{k_{34}}{k_{41}} N_3. \tag{34}$$

Accordingly, Eq. (7) for substrate flux in which N_4 is replaced by its value from Eq. (34) is now equivalent to Eq. (35).

$$\frac{d(X_i)}{dt} = k_{34} N_3. \tag{35}$$

The problem thus resumes at finding the expression for N_3 which can be obtained, in the case of model *4*, through the use of derived Eq. (18) and summation of Eqs. (10) and (11) in which the term $k_{43}N_4$ is dropped out such as to generate Eq. (36).

$$\frac{dN_2}{dt} + \frac{dN_3}{dt} = \frac{dN_3}{dt}\left[1 + \frac{K_2}{(X_o)}\right] = k_{12}N_1 - k_{21}N_2 - k_{34}N_3. \tag{36}$$

Since N_1 and N_2 can be expressed in terms of N_3 through the use of Eq. (1) (in which the N_4 term is dropped out) and (18), equations in N_3 similar to Eqs. (30) and (31) and for uptake similar to Eq. (32) can readily be obtained.

The same approximations as above hold for model *5* which can thus be solved by using Eq. (11) and taking into account Eqs. (1) and (17). The calculated values for A, B, and $1/\alpha$ corresponding to models *4* and *5* are shown in Tables 2–4. From Table 2, it is interesting to note that the amplitude term for model *5* can only be positive (lag) while model *4* may generate lag, burst, or no transient state.

The last case is represented by model *6* of Fig. 2 in which the two rapid steps are linked to substrate release on the internal side and where the reaction preceding the substrate-releasing step is in rapid equilibrium as defined by Eq. (19). Intermediary forms N_3 and N_4 thus need to be considered as a whole. Moreover, since the rate of decomposition of $(N_3 + N_4)$ is faster than its rate of formation, the steady-state treatment, as defined for models *4* and *5*, also applies in this case and Eq. (37) can be generated through the use of Eqs. (11), (12) and (19),

$$\frac{dN_3}{dt} + \frac{dN_4}{dt} = \frac{dN_4}{dt}[1 + K_3] = k_{23}(X_o)N_2 - k_{41}N_4 \approx 0. \tag{37}$$

It should be noted that the term $k_{32}N_3$ does not appear in Eq. (37) since k_{32} can be dropped out in front of k_{34} in Eq. (11) because it is much smaller in this model. Equation (37) thus allows us to write down Eq. (38) which, after introduction into Eq. (7), gives a new rate equation for substrate flux as defined by Eq. (39),

$$N_4 = \frac{k_{23}(X_o)N_2}{k_{41}} \tag{38}$$

$$\frac{d(X_i)}{dt} = k_{23}(X_o)N_2. \tag{39}$$

The problem thus reduces at finding the time dependence of N_2 which is readily obtained by using Eqs. (1) and (10). However, because of Eqs. (38) and (19), the concentrations of N_3 and N_4 are very small as compared to N_1 and N_2 and can be dropped out of Eq. (1). Also the term $k_{32}N_3$ being the product of a slow rate constant and a low concentration can be dropped out of Eq. (10), so that the transition from N_2 to N_3 is practically irreversible (dashed line in model *6* of Fig. 2). Equation (40) is thus obtained,

$$\frac{dN_2}{dt} = k_{12}N_1 - [k_{21} + k_{23}(X_o)]N_2. \tag{40}$$

Integration of Eq. (40) and then Eq. (39) leads to an equation similar in form to Eq. (32) with parameters A, B, and $1/\alpha$ as shown in Tables 2–4. It is obvious from Table 2 that such a model configuration can only generate a burst situation since the amplitude term is always negative.

Simulations

General Considerations

All simulations shown in this paper have been performed with model *4* of Fig. 2 because it corresponds to the most studied model of cotransport by the rapid equilibrium, steady-state approach (Schultz & Curran, 1970; Heinz et al., 1972; Jacquez, 1972; Kimmich & Carter-Su, 1978; Turner, 1981, 1983, 1985). It should be reminded that the main assumption in this model is that the rate-limiting steps in the transport process are the translocations of free and substrate-loaded forms of the carrier from one membrane face to the other, so that the transporters are in equilibrium with the ligands at the membrane surfaces. It should be emphasized however that similar simulations can be performed with any of the other models.

Simulations of zero-*trans* influx experiments have been performed using the rate constant values shown in Table 5. These have been arbitrarily chosen to generate lag situations over a time period compatible with our recent observations (Berteloot, 1986). The rule of microscopic reversibility was also preserved, i.e., the product of all clockwise rate constants is equal to the product of all counterclockwise ones. The carrier density was fixed at 10^{-7} mmol/mg protein and is compatible with that estimated from the equilibrium binding value of glutamic acid (Berteloot, 1984).

Validity of the Approximate Solutions

One may first question the validity of the hypothesis made in the above derivations of the rate equations for the approximate models with one transient state, particularly as to the pertinence of the steady-state approximation which was introduced to solve models *3–6* of Fig. 2. This problem is best answered by comparing the time variations in the concentrations of forms N_1–N_4 as estimated from the approximate analytical solutions obtained for model *4* with those calculated directly from the numerical integration of the general equations (9)–(12). The results of this comparison are shown in Fig. 3 from which it can be appreciated: (*i*) That the analytical and integrated solutions differ considerably during the early period of the fast relaxation processes (*see* insets of Fig. 3). (*ii*) That identical solutions are given by the two methods during the slow relaxation process with the exception of form N_4 (*see* Fig. 3*D*). In this case, however, it should be noted that this effect is only apparent due to the expanded scale used on the y-axis. Actually, only very low concentrations of this form are present during the slow relaxation process with values of N_4^o and N_4^S representing 0.0013 and 0.0045% of the total carrier concentration, respectively. On a practical point of view, this is not significantly different from zero, at least when compared to the other carrier forms N_1 (*see* Fig. 3*A*), N_2 (*see* Fig. 3*B*) and N_3 (*see* Fig. 3*C*) which represent 82.5–95.2%, 0.2–0.7% and 4.6–16.8% of the total carrier concentration, respectively. From these considerations, it is thus legitimate to eliminate the contribution of form N_4 from the conservation Eq. (1) during the derivation of model *4*. Also, since the overall variation with time in the concentration of N_4 is small, the values of dN_4/dt, which correspond to the slopes of the tangents determined at each time point along the concentration time curve for N_4 (*see* Fig. 3*D*), will also be small and not significantly different from zero, thus justifying the steady-state approach in the derivations of model *4*. (*iii*) That the concentration of form N_1 does not change significantly during the fast relaxation process (*see* inset of Fig. 3*A*), thus justifying the use of Eq. (20) to determine the zero time concentration of N_1 at the start of the relaxation process. (*iv*) That carrier forms N_2 and N_3 redistribute in opposite directions during the fast relaxation process (*see* insets of Fig. 3*B* and *C*) and that this redistribution satisfies Eqs. (18) and (23). The substrate uptake was also calculated numerically by integrating Eq. (7) and analytically using Eq. (32) with the appropriate expressions for model *4* given in Tables 2–4. The comparison of these results is shown in Fig. 4. Both uptake curves are confounded during the slow relaxation process and the difference between the two solutions can only be seen when using an expanded scale as shown in the inset where the uptake is expressed in fmol/mg protein.

Table 5. Numerical values of the rate constants used in the simulation experiments presented in Figs. 3–8

Rate constants
$k_{12}^o = 0.02$ (sec^{-1})
$k_{21}^o = 0.40$ (sec^{-1})
$k_{23}^o = 1362$ (sec^{-1} mM^{-1})
$k_{32}^o = 300$ (sec^{-1})
$k_{34}^o = 0.08$ (sec^{-1})
$k_{43}^o = 0.004$ (sec^{-1})
$k_{41}^o = 300$ (sec^{-1})
$k_{14}^o = 1362$ (sec^{-1} mM^{-1})

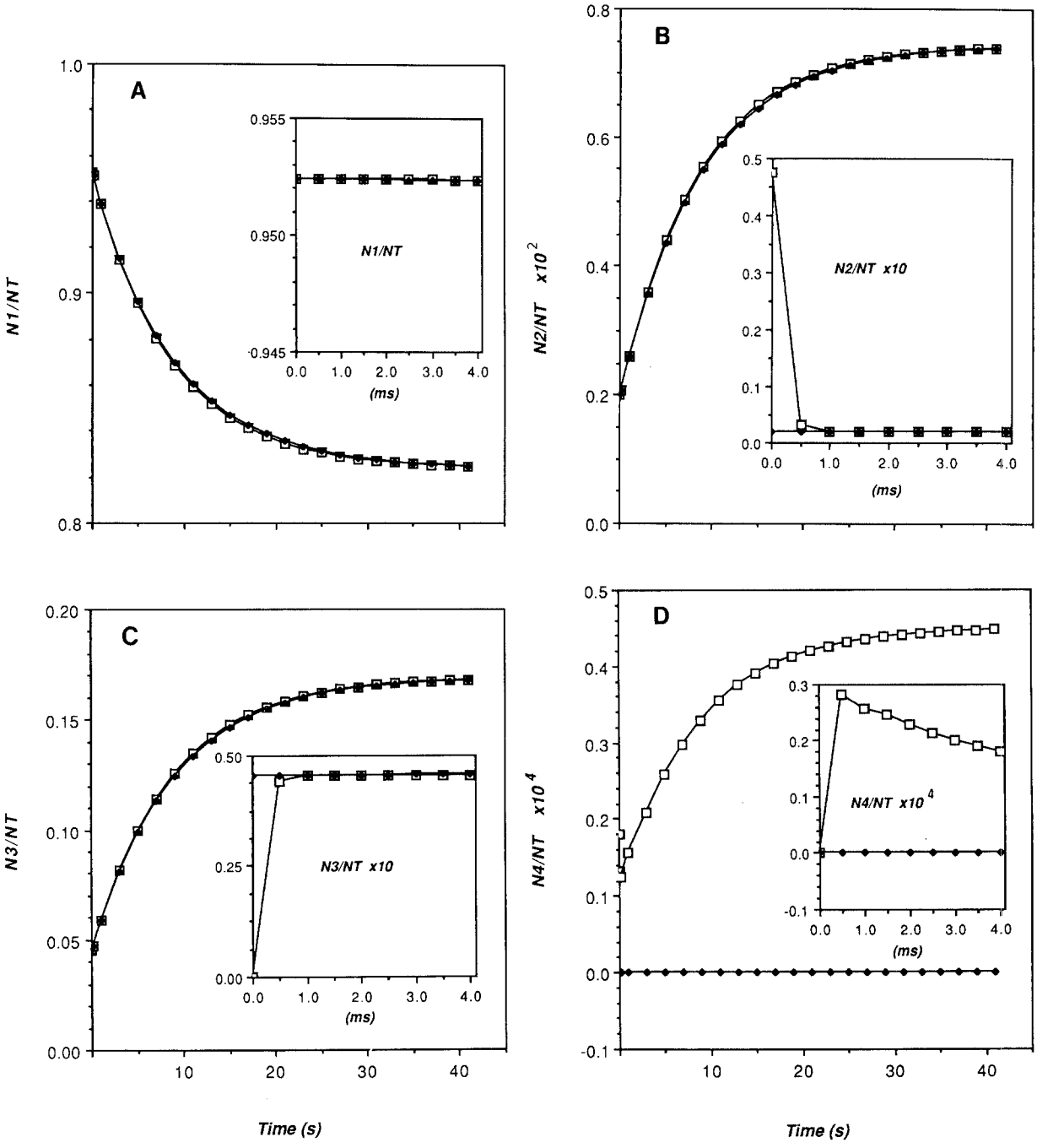

Fig. 3. Simulation of the time-dependent variations in the concentrations of intermediary carrier forms N_1 (*A*), N_2 (*B*), N_3 (*C*), and N_4 (*D*) during the fast (*insets*) and slow relaxation processes. Model *4* of Fig. 2 was used with rate constant values shown in Table 5. The membrane potential was set at 0 mV and the substrate concentration at 5 mM. The open and filled symbols show the results of the numerical and analytical calculations, respectively

A similar approach has also been used to justify the burst situation by permutating the values of the rate constants k_{12} and k_{21} and calculating k_{43} according to the rule of microscopic reversibility (*results not shown*). In the case of the other models of Fig. 2, the validity of the approximate analytical solutions derived in the previous section can also be assessed by comparison with the results of the numerical integration (*results not shown*). All together, these results thus support the approximations introduced in the derivation of the rate equations corresponding to the six models of Fig. 2.

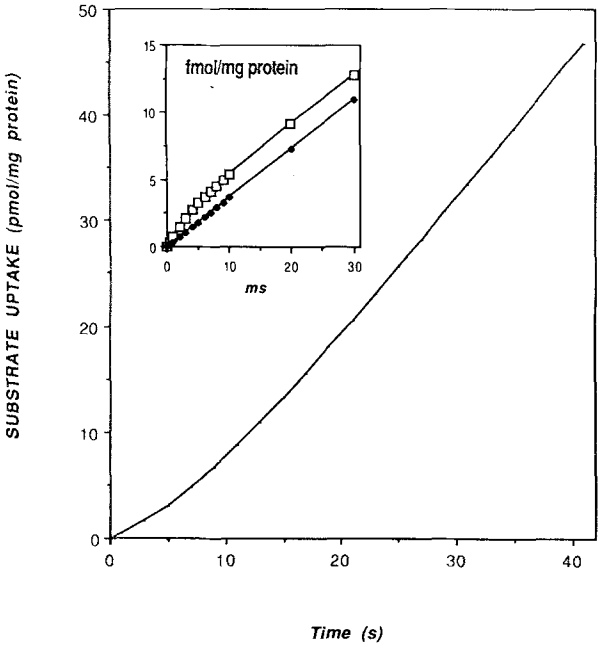

Fig. 4. Simulation of the time course of zero-*trans* uptake of substrate corresponding to the conditions of Fig. 3. The results obtained with the numerical (open symbol) and the analytical (filled symbol) calculations are shown in the inset using an expanded scale. Both results are confounded during the slow relaxation process

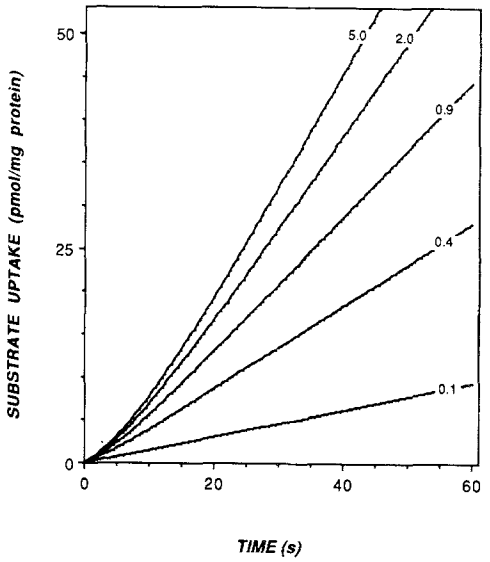

Fig. 5. Simulation of the time course of zero-*trans* uptake of substrate at fixed external substrate concentrations (mM) and with membrane potential clamped to zero. Values of the rate constants were as shown in Table 5 using model *4* of Fig. 2

Substrate Concentration Effects

The approximate solutions derived above allow, by simulation of the derived rate equations, to evaluate the influence of the substrate concentration on the transient kinetics. Such an example of a zero *trans* influx experiment was performed for model *4* of Fig. 2 using the expressions for A, B, and $1/\alpha$ as shown in Tables 2–4 with values for the rate constants as shown in Table 5. The corresponding uptake time courses are presented in Fig. 5 for substrate concentrations varying from 0.1 to 5 mM and in the absence of membrane potential. It is readily apparent from this figure that the transient state (lag) is more apparent with increasing substrate concentrations. That this effect is due to an increase in both the amplitude and the time constant of the relaxation can be better seen from the curves pertaining to the 0 mV situation in Fig. 7*B* and *C*, respectively. At the same time, the steady-state rate of substrate accumulation is also increased (*see* Fig. 5) and follows the expected Michaelian behavior (*see* Fig. 7*A* at 0 mV). This result contrasts with the substrate dependency of the amplitude which clearly shows a non-Michaelian profile (sigmoidicity) over the same range of concentrations (*see* Fig. 7*B*).

It should be emphasized that similar simulations can be performed on this model under burst situations. In this case, the amplitude of the transient state increases with increasing substrate concentrations, but becoming more and more negative. However, the value of the time constant decreased with increasing substrate concentrations (*results not shown*).

The same effects of increased substrate concentrations are expected for model *1* of Fig. 2 which can also lead to either lag or burst situations. Since in both cases the sign of the amplitude is independent of the substrate concentration as shown in Eqs. (1) and (4) of Table 3, it can be concluded that lag-to-burst transitions are never to be expected in such models by varying the external substrate concentration.

While simulations of substrate concentration effects could as well be performed for all models of Fig. 2, it is not necessary to do so in order to assess the validity of such an experimental approach aiming at model discrimination. By just looking at the form of the substrate dependency predicted by the equations for A and $1/\alpha$ corresponding to each of these models (*see* Tables 2 and 4), it can be readily appreciated that concurrent models may indeed be differentiated from the analysis of the substrate effects on these experimentally determinable parameters. Thus, while models *1*, *2*, *4* and *6* should present saturation in A with increasing substrate concentrations, the two other models will show a

continuous decrease of this parameter under similar conditions (*see* Table 2). Similar observations apply to $1/\alpha$. While saturating functions are to be expected for models *1, 2* and *4*, a continuous decrease should be observed with the three other models (*see* Table 4). It is noteworthy in the context of the present discussion that the expressions for the steady-state influx B only show saturation with substrate concentrations for all models (Table 3), thus clearly supporting the view that the steady-state approach alone will not in general allow any conclusion to be drawn as to the localization of the rate-limiting steps along a given transport pathway. However, when considering the substrate dependency of A and $1/\alpha$, it appears possible to discriminate between models (*1, 2* and *4*), (*3–5*), and *6*. Moreover, since the equations for A, B, and $1/\alpha$ pertaining to each model are analytically expressed in terms of the rate constants for the rate-limiting steps and of the equilibrium constants for the fast ones, all of these may actually be determined from experimental results obtained at different ligand concentrations using standard curve-fitting procedures on these experimental parameters. This clearly shows both the interest and the power of the presteady-state approach as compared to the steady-state one.

Membrane Potential Effects

The approximate solutions derived above also allow, by simulation of the derived equations, to evaluate the influence of the membrane potential on the transient kinetics. Of particular concern to us in this regard was to evaluate the possibility for membrane potential-induced transitions from lag to burst, in order to assess the relevancy of the suggestion made in the introduction that the shift from upward to downward deviations as seen in the uptake of glutamic acid by rabbit intestinal brush-border membrane vesicles may actually be compatible with the observation of presteady-state kinetics. For this purpose, we choose again to simulate the equations corresponding to model *4* of Fig. 2. This choice was not done arbitrarily since, in order to observe a transition from burst to lag, one needs a model in which the expression for the A term can change its sign, so that only models *1* and *4* can satisfy this criterion.

To evaluate the membrane potential effects on the transient kinetics of model *4* in terms of possible transitions from lag to burst, we only need to consider the difference $(k_{21} - k_{34})$ which appears in the derived expression of the amplitude, in accordance with Eq. (4) of Table 2. The membrane potential effect is then introduced in these rate constants according to the formalism and symbolism recently developed by Läuger and Jauch (1986). The two rate constants can thus be written as Eq. (41) and (42).

$$k_{21} = k_{21}^o \, e^{-(z_L\delta+\eta)\frac{u}{2}} \tag{41}$$

$$k_{34} = k_{34}^o \, e^{-[(z_L+z_x)\delta+\eta]\frac{u}{2}}. \tag{42}$$

In these equations, z_x and z_L represent the charges present on the substrate and the empty carrier, respectively, δ is the fractional dielectric distance over which these charges move, and η is the dielectric distance over which additional charge displacements may occur during a conformational transition that leads to reorientation of polar residues other than the substrate binding site. Also, in these equations, k_{21}^o and k_{34}^o are the values of the rate constants in the absence of membrane potential and u is given by Eq. (43),

$$u = \frac{FV}{RT} \tag{43}$$

where V is the membrane potential difference between the internal and external compartments and where F, R and T have their usual meanings.

It is now possible to write down the difference between these two rate constants which can be cast under the form of Eq. (44) after a few simple transformations.

$$k_{21} - k_{34} = e^{-(z_L\delta+\eta)\frac{u}{2}}\left[k_{21}^o - k_{34}^o e^{-z_x\delta\frac{u}{2}}\right]. \tag{44}$$

Under this form, Eq. (44) clearly shows that lag-to-burst transitions (or the reverse) are actually possible with such a model provided that z_x and/or δ are not equal to zero. This last condition is rather interesting since it eliminates models where the inside-to-outside conformational transitions are voltage independent, that is in the so-called "high-field access-channels" or "ion wells." Also, Eq. (44) clearly indicates that reversal of the sign of the amplitude of the transient state is independent of the presence of charges on the free carrier, whether at the substrate binding site or not. Finally, for such transitions to be observed on a physiological range of membrane potentials, it can be seen from Eq. (44) that the values of k_{21}^o and k_{34}^o need to be of the same order of magnitude.

For these reasons, the simulation of lag-to-burst transitions was done using the values of the rate constants shown in Table 5 with a value for δ set equal to 1, that is in the case of a "low-field access-channel" where the access channel is a wide aque-

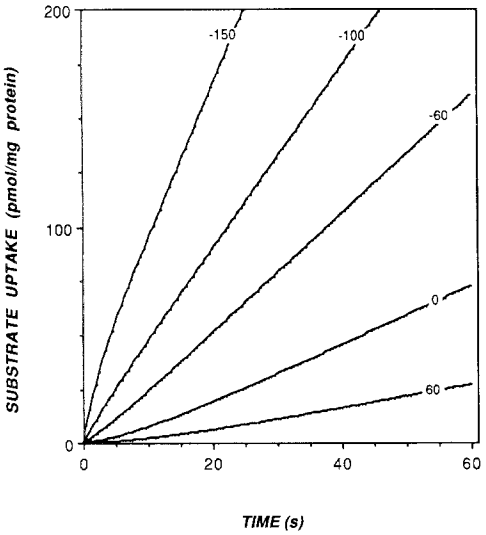

Fig. 6. Simulation of the time course of zero-*trans* uptake of substrate at varying membrane potentials (mV) and fixed substrate concentration of 5 mM. Values of the rate constants were as shown in Table 5 using model *4* of Fig. 2

ous pore or vestibule with a low electric resistance so that the whole membrane potential effect occurs on the inside-to-outside conformational transitions of the empty and loaded carrier forms. Also, the value of η was set at 0.5 (Läuger & Jauch, 1986) and the substrate concentration at 5 mM. Figure 6 shows the result of such a simulation with values for z_x and z_L of $+1$ and -1, respectively, so that the loaded complex is neutral. Such a situation was chosen to mimick glutamic acid transport through the binding of 1 glutamate$^-$ and 2 Na^+ ions on a negatively charged carrier (Burckhardt et al., 1980; Schneider & Sacktor, 1980; Nelson et al., 1983; Himukai, 1984; Fukuhara & Turner, 1985; Rajendran et al., 1987; Wingrove & Kimmich, 1987). It can thus be concluded that lag-to-burst transitions can be generated under these conditions when going from inside-positive to inside-negative membrane potentials.

The effect of varying the substrate concentration at different values of the membrane potential was also simulated and the results of this study are shown in Fig. 7 for the different measurable parameters relating to substrate uptake. It is interesting to note that saturation with substrate concentration is observed at all membrane potentials for the steady-state influx B (Fig. 7*A*) as well as for the amplitude A (Fig. 7*B*) and the time constant $1/\alpha$ (Fig. 7*C*) of the transient state. However, the non-Michaelian behavior of the amplitude as compared to both the steady-state influx and the time constant should again be emphasized. Also, the opposite effects of the substrate concentration in increasing or decreasing the time constant of the transient state dur-

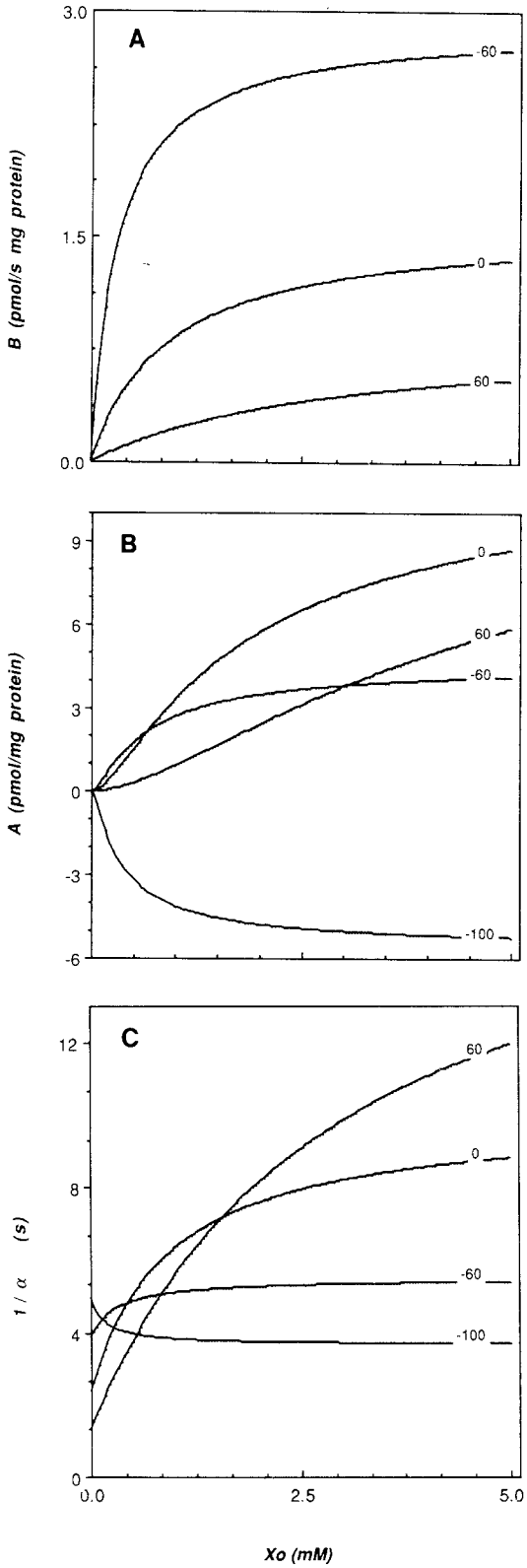

Fig. 7. Simulation of the effect of varying substrate concentrations at fixed membrane potential values (mV) on the steady-state influx (*A*), the amplitude (*B*) and the time constant (*C*) of the transient state. Values of the rate constants were as shown in Table 5 using model *4* of Fig. 2

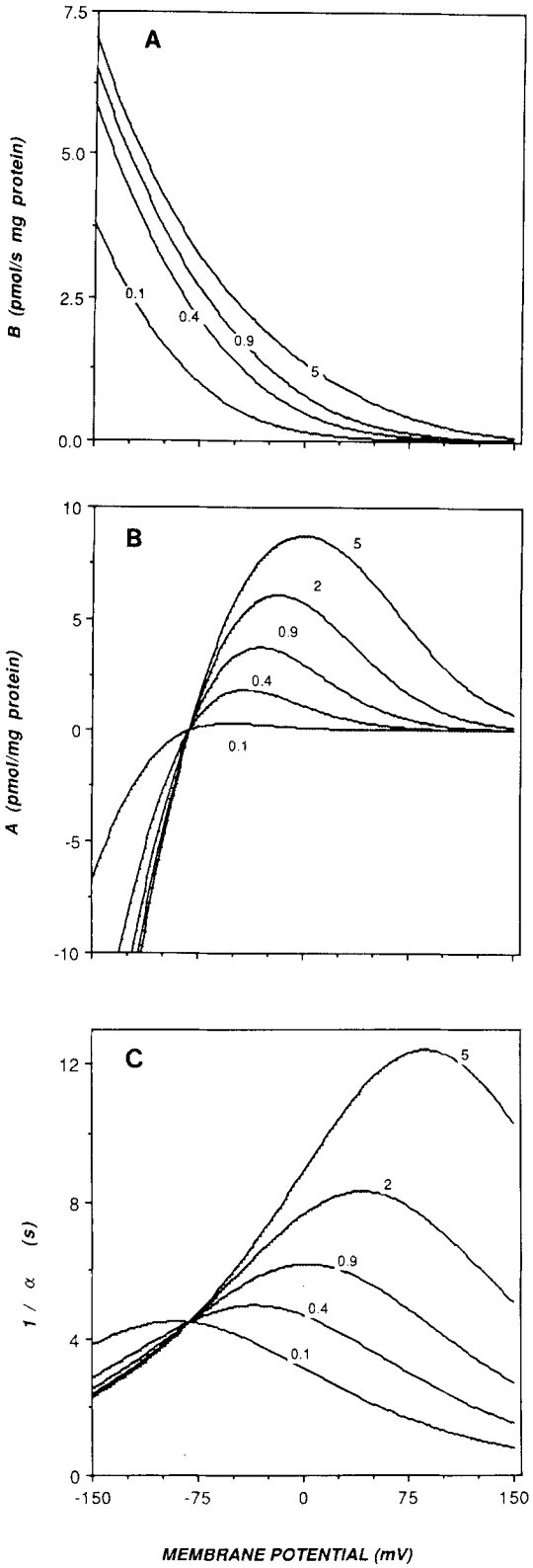

Fig. 8. Simulation of the effect of varying membrane potentials at fixed substrate concentrations (mM) on the steady state (*A*), the amplitude (*B*) and the time constant (*C*) of the transient state. Values of the rate constants were as shown in Table 5 using model *4* of Fig. 2

ing lag and burst situations, respectively, is worth noting in Fig. 7*C*. As can be better appreciated in Fig. 8*A–C*, all of the measurable parameters are complex functions of the membrane potential which are highly dependent on the substrate concentration. Also, Fig. 8*B* clearly demonstrates that the sign of the amplitude of the transient state (lag-to-burst transitions) can only be reversed by changing the polarity of the membrane potential and is independent of the substrate concentration.

Simulations similar to those above could as well be performed with any of the other models. Obviously, from the equations of the relaxation amplitudes shown in Table 2, only model *1* may be expected to generate a lag-to-burst transition. However, the membrane potential dependency of this parameter will be more complex due to the presence of the equilibrium constant K_3 in the expression influencing the sign of this parameter and many cases may need to be considered. As to the other models, the expressions for the membrane potential dependency of the different experimental parameters will obviously be quite complex also such as to preclude any relevant information to be gained in terms of model discrimination without further simplifications.

Discussion

In this paper, we fully describe for the first time the presteady-state kinetics of carrier-mediated transport under zero-*trans* conditions and demonstrate that the number of transient states to be observed depends on the number p of intermediary steps involved in the substrate flux pathway and is equal to $(p - 1)$. It should be emphasized, however, that this conclusion may only be valid for transport models in which the fully loaded form of the carrier is the only pathway involved in the transmembrane permeation of the substrate since the presence of internal leaks (slip) and branched pathways were not evaluated in our derivations. It should also be emphasized that the derivation of the analytical expressions for both the amplitude and the time constant of the different relaxations is not possible for models with $p > 5$, a situation which is already attained with the even simplest model of cotransport represented by a six-state transport mechanism. We thus aimed at finding the analytical expressions of these experimental parameters for such models by introducing realistic simplifications which were tested in the simpler case of the four-state, carrier-mediated transport mechanism.

The simplest hypothesis that would reduce the number of observable transient states is based on

the time-scale separation hypothesis which simply states that all transitions between the elementary reactions leading to substrate flux do not proceed at the same rate, so that only the slowest ones can be seen in realistic experiments. This principle was applied to the four-state model of carrier-mediated transport by assuming that only one transient state could be observed. It should be stressed that this condition is not restrictive for the application of the method which could easily be extended to a higher number of observed relaxations. However, in such cases, polynomials of degree 2 or 3 may need to be solved.

Under these conditions, we show that the general four-state model of carrier-mediated transport leads to six degenerate models depending on the relative positions of two rate-limiting steps along the transport pathway. It is then possible to derive the flux equations for each of these by integration of only one differential equation. From the detailed study of each particular case and the justification of the validity of the derived analytical expressions which were presented in Results, it seems that this approach can now be generalized as the "rapid equilibrium (presteady-state) approximation" with the following rules:

(*i*) All of the intermediary states which are linked by rapid steps can be described by equilibrium constants. In the generalized treatment which is proposed here, this also includes the rapid step which leads to internal liberation of substrate, so that Eq. (45) needs to be considered.

$$K_4 = \frac{(X_i)N_1}{N_4}. \tag{45}$$

Obviously, in models *4* to *6* of Fig. 2, Eq. (45) will lead directly to the conclusion that $N_4 = 0$ and the concentration of this carrier form can be dropped out of the conservation Eq. (1). Moreover, when combining rapid steps leading to the internal liberation of substrate, all the concentrations of the intermediary forms involved will become equal to zero and can then be neglected in the conservation equation. This can be easily verified in the case of model *6* by combining Eq. (19) and (45).

(*ii*) In analogy with the rapid equilibrium, steady-state treatment of transport mechanisms, the substrate flux equation is governed by the first slow transition preceding the internal substrate release step. Moreover, since zero-*trans* conditions prevail, this step can be considered as irreversible. This conclusion can be easily verified by inspection of the six models of Fig. 2.

(*iii*) The differential equation which governs the time dependence of the carrier form involved in the substrate flux equation is easily found from the derivative of the conservation equation in which all negligible concentrations of intermediary carrier forms have been dropped out according to rule *i* and in which all intermediary forms still linked by rapid steps have been grouped. This can easily be verified from the differential equations pertaining to each of the models of Fig. 2. Moreover, under its differential form, this equation automatically gives the analytical expressions for the steady-state concentration N_j^S of the carrier form involved in the rate law for substrate release and for the time constant of the relaxation process ($1/\alpha$).

(*iv*) The differential equation obtained under rule *iii* can now be integrated with an upper boundary condition given by N_j^S and a lower boundary condition given by the concentration N_j^o of the carrier form involved in the rate law for substrate release which was present following the rapid redistribution of the carrier forms involved in the true initial conditions N_j^*. The N_j^* are easily determined from the known preincubation conditions while the N_j^o are calculated by considering the rapid steps connecting the N_j^* and the N_j^o.

(*v*) Finally, the substrate rate law can be integrated in order to find out the analytical expression of the relaxation amplitude (A).

It should be emphasized that these rules are also expected to apply to more complex models involving any number of intermediary steps.

In the case of the four-state mechanism for carrier-mediated transport, this simple treatment allows very interesting conclusions to be reached and allows establishment of the following experimental criteria for model discrimination:

(*i*) The type of relaxation (lag and/or burst) is strongly dependent upon the relative positions of the rate-limiting steps along a given transport cycle. Actually, lags can be generated in all types of models except for model *6* in which both the recycling of the free carrier and the outside ligand binding step are rate limiting. On the other hand, bursts can only be generated in models where the recycling of the free carrier is one of the rate-limiting steps (models *1*, *4* and *6*). Only two models (*1* and *4*), including the most studied rapid equilibrium steady-state model *4* (Schultz & Curran, 1970; Heinz et al., 1972; Jacquez, 1972; Kimmich & Carter-Su, 1978; Turner, 1981, 1983, 1985), show rather flexible kinetics as they will accommodate either lags or bursts or absence of transient state. From an experimental point of

view, it can thus be concluded that the direct observation of lags and bursts are necessary conditions that would allow rejection of model *6* and models *2, 3* and *5*, respectively. It should be noted, however, that the absence of presteady-state, while compatible with models *1* and *4*, cannot be differentiated from true steady state without further experimentation.

(*ii*) The substrate dependency of the analytical expressions for the experimentally measurable parameters of the uptake transient states (A and $1/\alpha$) is different according to the different configurations of the rate-limiting steps. Accordingly, as discussed in more details in Results, it seems possible to discriminate between models (*1, 2* and *4*), (*3* and *5*) and *6* by such an experimental analysis. Also, it can be concluded that variations in the substrate concentrations may help in modulating both the amplitude and the time constant of the transient state but that transitions from lag-to-burst kinetics cannot be induced by changing the substrate concentration in the simple carrier mechanism. Finally, it is important to emphasize that the substrate dependency of the relaxation amplitude is always non-Michaelian in nature since involving square terms in substrate concentration in the denominator (always) and the numerator (sometimes) of its analytical expression. It is interesting to point out that the results of Otsu et al. (1989) demonstrate the presence of a sigmoid (non-Michaelian) dependence of the burst amplitude on the Na^+ concentration. In our model calculation, such a dependence is expected and does not require additional assumptions such as multiple interacting sites as suggested by Otsu et al. (1989).

(*iii*) Studies analyzing the effect of membrane potential on presteady-state kinetics can be useful to modulate the substrate concentration dependency of such transport kinetics. Obviously, such studies are only possible with charged substrates and/or carriers. In this last case, it is interesting to note that nonrheogenic transport pathways may, however, show membrane potential sensitivity during the presteady-state period. Also, it should be noted that membrane potential-induced transitions from lag-to-burst kinetics are only possible with two of the six models of Fig. 2 (models *1* and *4*) and thus that such an observation can be used as an absolute criterion in favor of any of these two models.

(*iv*) Experimental results can be compared to the predictions of a specific model and, in general, all of the rate and equilibrium constants may be estimated by standard curve-fitting procedures. It is interesting to note, however, that the carrier concentration, which is usually determined from the value of the burst amplitude in enzyme kinetics, is not directly attainable from this expression without knowing (or having determined first) the values of the other parameters describing the model. It should also be mentioned that models *1* and *4* on one hand, and models *3* and *5* on the other hand, cannot be differentiated based on zero-*trans* influx experiments alone. However, assuming that presteady-states could also be observed in zero-*trans* efflux experiments, then, because of symmetrical considerations, models *1* and *5* should now behave like models *6* and *2*, respectively, while the behavior of models *3* and *4* should not be changed. It thus seems possible to select one particular approximate model and thus to determine the rate-limiting steps along a transport pathway by an adequate choice of experimental conditions.

It is important to emphasize that the above conclusions may not apply to more complex transport mechanisms. For example, conclusion (*i*) is particularly obvious in the special case of only one transient state being observed and should apply as well to more complicated cases. However, increasing the number of the rate-limiting steps will also complicate the shape of the uptake transients as successions of lag(s) and/or burst(s) may be anticipated. Such a situation may well be compatible with the observations of Otsu et al. (1989) with the Na^+-H^+ exchanger of rabbit renal brush-border membranes. Also, the conclusion that transitions from lag-to-burst kinetics cannot be induced by changes in the substrate concentration do not seem to apply to a six-state model of cotransport even when assuming rapid equilibrium at the surfaces as shown by theoretical studies actually in progress. Nevertheless, the fact that such transitions can be observed when varying the membrane potential does support the hypothesis made in the introduction as to the observation of presteady-state kinetics in the transport of glutamic acid by rabbit jejunal brush-border membrane vesicles (Berteloot, 1986).

In summary, our demonstration that even complex cotransport models can lead to the derivation of approximate solutions and analytical equations should be viewed as an invitation to develop new techniques that would allow a more straightforward analysis. Such an effort has been made in our laboratory over the last 2 years and should give us an opportunity to critically evaluate soon our preliminary data with glutamic acid uptake.

This research was supported by operating grant MA-7607 from the Medical Research Council of Canada (A.B.) and A-5807 from the Natural Sciences and Engineering Research Council of Can-

ada (G.R.). One of the authors (A.B.) received a scholarship from the "Fonds de la Recherche en Santé du Québec" while an other (W.W.) received a studentship from "Formation de Chercheurs et Aide à la Recherche". The authors thank Miss Lise Imbeault for her secretarial help, and G. Filosi, C. Gauthier and D. Cyr for the artwork.

References

Berteloot, A. 1984. Characteristics of glutamic acid transport by rabbit intestinal brush-border membrane vesicles. Effects of Na^+, K^+-, and H^+-gradients. *Biochim. Biophys. Acta* **775:**129–140

Berteloot, A. 1986. Membrane potential dependency of glutamic acid transport in rabbit jejunal brush-border membrane vesicles: K^+ and H^+ effects. *Biochim. Biophys. Acta* **861:**447–456

Burckhardt, G., Kinne, R., Stange, G., Murer, H. 1980. The effect of potassium and membrane potential on sodium-dependent glutamic acid uptake. *Biochim. Biophys. Acta* **599:**191–201

Crane, R.K. 1977. The gradient hypothesis and other models of carrier-mediated active transport. *Rev. Physiol. Biochem. Pharmacol.* **78:**99–159

Crane, R.K., Dorando, F.C. 1984. On the mechanism of Na^+-dependent glucose transport. *Ann. NY Acad. Sci.* **339:**46–52

Dorando, F.C., Crane, R.K. 1984. Studies on the kinetics of Na^+ gradient coupled glucose transport as found in brush-border membrane vesicles from rabbit jejunum. *Biochim. Biophys. Acta* **772:**273–287

Fukuhara, Y., Turner, R.J. 1985. Cation dependence of renal outer cortical brush border membrane L-glutamate transport. *Am. J. Physiol.* **248:**F869–F875

Geck, P., Heinz, E. 1981. Coupled transport of metabolites. *In:* Membrane Transport. S.L. Bonting and J.J.H.H.M. de Pont, editors. Vol. 2, Chap. 11, pp. 285–310. Elsevier, North-Holland

Hammes, G.G., Schimmel, P.R. 1970. Rapid reactions and transient states. *In:* The Enzymes. P.D. Boyer, editor. pp. 67–114. Academic, New York

Harrison, D.A., Rowe, G.W., Lumsden, C.J., Silverman, M. 1985. Computational analysis of models for cotransport. *Biochim. Biophys. Acta* **774:**1–10

Heinz, E., Geck, P., Wilbrandt, W. 1972. Coupling in secondary active transport. Activation of transport by cotransport and/or countertransport with the fluxes of other solutes. *Biochim. Biophys. Acta* **255:**442–461

Himukai, M. 1984. Rheogenic property of Na^+/acidic amino acid cotransport by guinea pig intestine. *Jpn. J. Physiol.* **34:**815–826

Hopfer, U. 1977. Kinetics of Na^+-dependent D-glucose transport. *J. Supramolec. Struct.* **7:**1–13

Hopfer, U., Groseclose, R. 1980. The mechanism of Na^+-dependent D-glucose transport. *J. Biol. Chem.* **255:**4453–4462

Hopfer, U., Nelson, K., Perrotto, J., Isselbacher, K.J. 1973. Glucose transport in isolated brush border membrane from rat small intestine. *J. Biol. Chem.* **248:**25–32

Jacquez, J.A. 1972. Models of ion and substrate cotransport and the effect of membrane potential. *Math. Biosci.* **13:**71–93

Kimmich, G.A., Carter-Su, C. 1978. Membrane potentials and the energetics of intestinal Na^+-dependent transport systems. *Am. J. Physiol.* **235:**C73–C81

Laprade, R., Ciani, S.M., Eisenman, G., Szabo, G. 1975. The kinetics of carrier mediated ion permeation in lipid bilayers and its theoretical interpretation. *In:* Membranes: G. Eisenman, editor. Vol. 3, pp. 127–241. Marcel Dekker, New York

Läuger, P., Jauch, P. 1986. Microscopic description of voltage effects on ion-driven cotransport systems. *J. Membrane Biol.* **91:**275–284

Nelson, P.J., Dean, G.E., Aronson, P.S., Rudnick, G. 1983. Hydrogen ion cotransport by the renal brush border glutamate transporter. *Biochemistry* **22:**5459–5463

Otsu, K., Kinsella, J., Sacktor, B., Froehlich, J.P. 1989. Transient state kinetic evidence for an oligomer in the mechanism of Na^+-H^+ exchange. *Proc. Natl. Acad. Sci. USA* **86:**4818–4822

Rajendran, V.M., Harig, J.M., Adams, M.B., Ramaswamy, K. 1987. Transport of acidic amino acids by human jejunal brush-border membrane vesicles. *Am. J. Physiol.* **252:**G33–G39

Sanders, D. 1986. Generalized kinetic analysis of ion-driven cotransport systems: II. Random ligand binding as a simple explanation for non-Michaelian kinetics. *J. Membrane Biol.* **90:**67–87

Sanders, D., Hansen, U.-P., Gradmann, D., Slayman, C.L. 1984. Generalized kinetic analysis of ion-driven cotransport systems: A unified interpretation of selective ionic effects on Michaelis parameters. *J. Membrane Biol.* **77:**123–152

Schneider, E.G., Sacktor, B. 1980. Sodium gradient-dependent L-glutamate transport in renal brush border membrane vesicles. Effect of an intravesicular > extravesicular potassium gradient. *J. Biol. Chem.* **255:**7645–7649

Schultz, S.G., Curran, P.F. 1970. Coupled transport of sodium and organic solutes. *Physiol. Rev.* **50:**637–718

Semenza, G., Kessler, M., Hosang, M., Weber, J., Schmidt, U. 1984. Biochemistry of the Na^+, D-glucose cotransporter of the small-intestinal brush border membrane. The state of the art in 1984. *Biochim. Biophys. Acta* **779:**343–379

Stark, G., Ketterer, B., Benz, R., Laüger, P. 1971. The rate constants of valinomycin-mediated ion transport through thin lipid membranes. *Biophys. J.* **11:**981–994

Stein, W.D. 1976. An algorithm for writing down flux equations for carrier kinetics, and its application to cotransport. *J. Theor. Biol.* **62:**467–478

Stein, W.D., Honig, B. 1977. Models for the active transport of cations. The steady state analysis. *Mol. Cell. Biochem.* **15:**27–44

Turner, R.J. 1981. Kinetic analysis of a family of cotransport models. *Biochim. Biophys. Acta* **649:**269–280

Turner, R.J. 1983. Quantitative studies of cotransport systems: Models and vesicles. *J. Membrane Biol.* **76:**1–15

Turner, R.J. 1985. Solution of carrier-type transport models: General solution for an arbitrarily complex rapid equilibrium model. *J. Membrane Biol.* **88:**77–83

Widdas, W.F. 1952. Inability of diffusion to account for placental glucose transfer in the sheep and consideration of the kinetics of a possible carrier transfer. *J. Physiol. (London)* **118:**23–29

Wingrove, T.G., Kimmich, G.A. 1987. High affinity L-aspartate transport in chick small intestine. *Am. J. Physiol.* **252:**C105–C114

Received 13 November 1989; revised 6 February 1990